Chemical Science
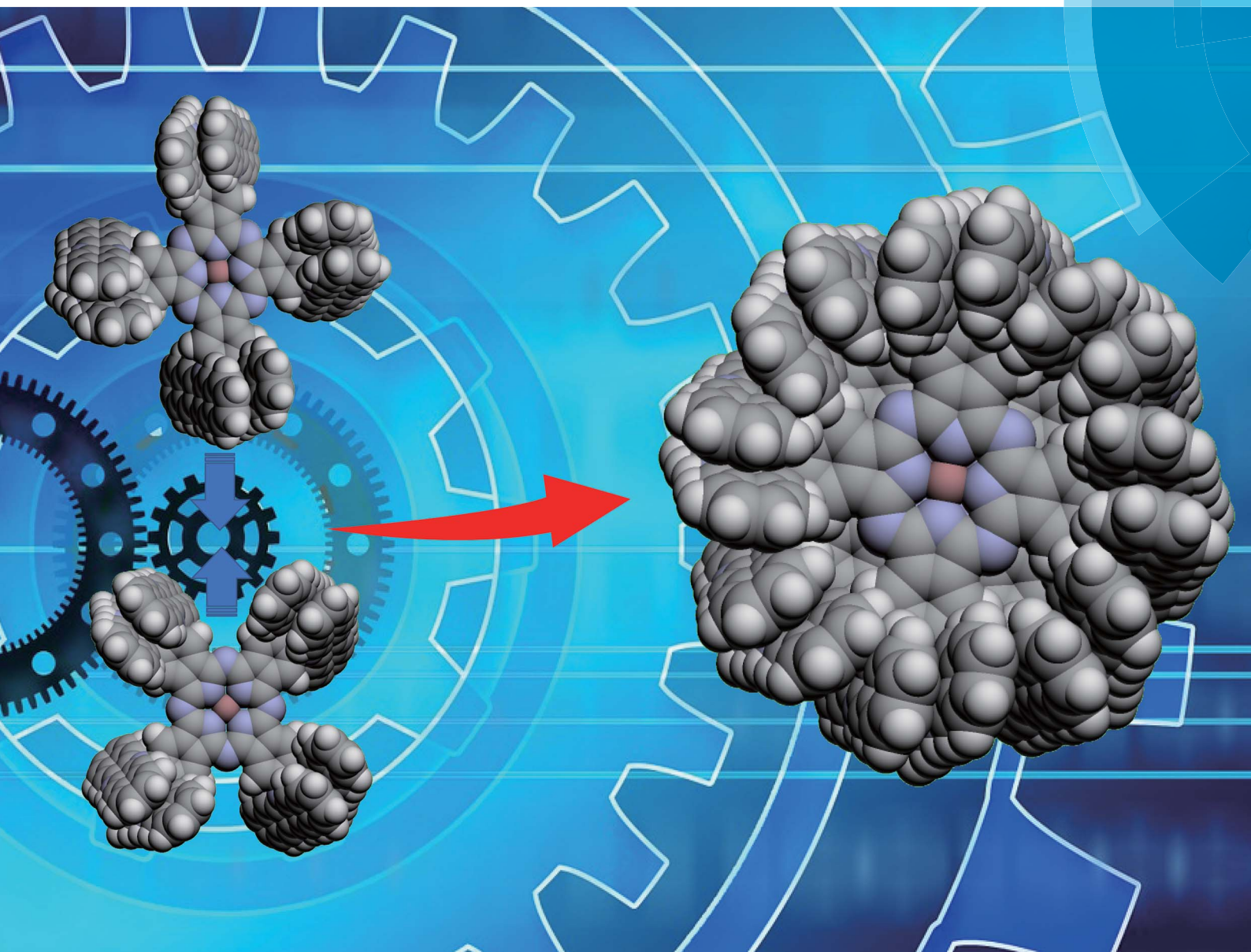
rsc.li/chemical-science

ROYAL SOCIETY OF CHEMISTRY | Celebrating IYPT 2019

EDGE ARTICLE
Daisuke Sakamaki, Shu Seki *et al.*
Extreme multi-point van der Waals interactions: isolable dimers of phthalocyanines substituted with pillar-like azaacenes

Check for updates

Extreme multi-point van der Waals interactions: isolable dimers of phthalocyanines substituted with pillar-like azaacenes†

Hidenori Saeki,[a] Daisuke Sakamaki,*[ab] Hideki Fujiwara [ID] [b] and Shu Seki [ID] *[a]

How strong are van der Waals interactions in determining the final outcome of self-assembled structures of small molecular systems? Herein we report isolable phthalocyanine (Pc) dimers bound by $\pi-\pi$ interactions between monomeric Pcs which can be handled as single entities. Pc dimers have been continuously investigated as one of the simplest models of Pc aggregates. Pcs were substituted with eight dihydrodiazapentacene (DHDAP) moieties on the periphery, which act as pillar-like π-planes and these molecules form H-type dimers with the help of synergetic $\pi-\pi$ interactions between two co-facial Pc rings and among the pillar-like DHDAP moieties. The dimer structures were fully confirmed by 1D and 2D NMR, ESR, and electronic absorption measurements. The dissociation of these dimers was observed in particular solvents such as *o*-dichlorobenzene, due to the good solubility of the larger π-conjugated molecules. On the other hand, in ethyl acetate the monomers were metastable species and underwent selective dimerization. Interestingly in THF, neither the dimerization of the monomers nor the dissociation of dimers was observed, suggesting that both the dimers and the monomers were kinetically well stabilized. For hours to days, we can handle these dimers as "a molecule" not only in solution but also even in mass spectrometry under ionization conditions without significant dissociation.

Introduction

Phthalocyanines (Pcs) are one of the special classes of functional dyes and pigments due to their high photostability and wide range of applications.[1,2] The photophysical properties of dye aggregates differ considerably due to the relative arrangement of dye molecules,[3] leading to different types of exciton coupling.[4] Hence, it is important and challenging to control the mode of aggregation of dye molecules. Until now, various kinds of Pc derivatives have been synthesized and their aggregates were investigated to understand the relationship between the relative arrangement of the Pcs and the electronic properties.[5–8] In particular, as the simplest model of Pc aggregates, various Pc dimers have been intensively studied.[9] In the pioneering studies on covalently bound Pc dimers, Leznoff, Lever and coworkers reported tethered Pc dimers, which can stack in a "clamshell" fashion.[10–13] After these studies, various covalently linked Pc dimers were reported, where Pcs were differently arranged such as in a coplanar,[14–16] cofacial (**A** in Fig. 1a),[17,18] and slipped-stack

manner.[19] In 1986, three independent research groups consecutively reported the selective dimerization of Pcs by means of metal complexation using Pc (**B** in Fig. 1a) substituted by four crown ether moieties (15-crown-5), which form co-facial dimer (H-type) triggered by the addition of cations such as alkaline or alkaline earth metal cations (Fig. 1a).[20–22] The dimerization of these "crowned" Pcs proceeds in a two-step manner upon gradual addition of specific cations; at the first stage, linear dimers are formed which share one guest cation and are then converted to co-facial dimers by capturing additional cations.[23] Due to high directionality and binding strength of coordination bonds, various other Pc dimers based on metal–ligand interactions have been designed.[24–27] Other intermolecular interactions such as hydrogen bonds[28,29] or hydrophobic forces[30] have been also adopted as the driving force for the selective dimerization of Pcs. In this context, $\pi-\pi$ interactions[31] are also considered as an important intermolecular force to control molecular assembly of Pcs because of their large π plane.[32] A few examples are reported for the selective dimerization of Pcs using $\pi-\pi$ interactions; however it is difficult to avoid the formation of higher aggregates. In 1993, Kobayashi *et al.* reported that a Pc substituted with two enantiopure 2,2′-dihydroxy-1,1′-binaphthyl at the periphery of the Pc ring is in equilibrium between the monomer and the co-facial dimer in solution.[33] Jiang *et al.* also reported the co-facial dimerization of the Pc with four 2,2′-dihydroxy-1,1′-binaphthyl groups, and they

[a]Department of Molecular Engineering, Graduate School of Engineering, Kyoto University, Nishikyo-ku, Kyoto 615-8510, Japan. E-mail: seki@moleng.kyoto-u.ac.jp
[b]Department of Chemistry, Graduate School of Science, Osaka Prefecture University, Naka-ku, Sakai-shi, Osaka 599-8531, Japan. E-mail: sakamaki@c.s.osakafu-u.ac.jp
† Electronic supplementary information (ESI) available. See DOI: 10.1039/c9sc01739a
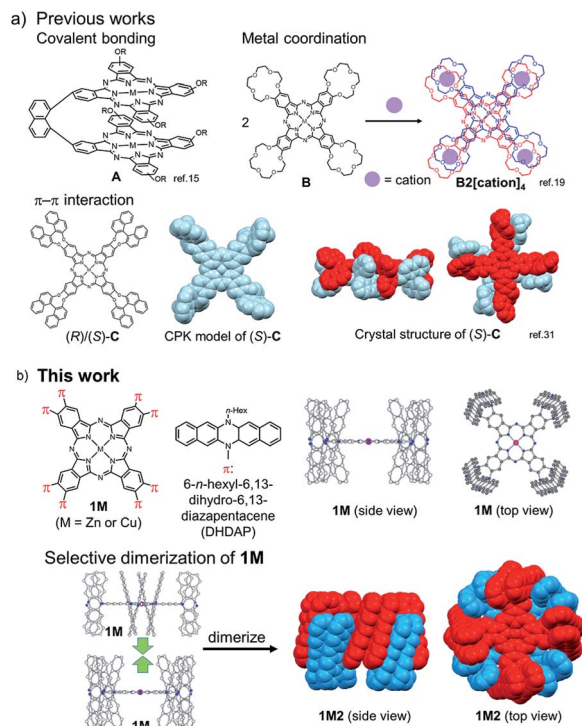
Fig. 1 (a) Previous examples of cofacially stacked Pc dimers bound by covalent bonding, metal coordination, and π−π interactions. (b) Molecular structure of Pcs with eight diazapentacene moieties (**1M**) and the schematic representation of the formation of the dimers (**1M2**).

revealed the dimer structures by X-ray single crystal analysis, indicating the presence of multiple π−π interactions between the two Pc planes and among the peripheral binaphthyl substituents (**C** in Fig. 1a).[34] However, in these cases, the separation of the monomer and the dimer was not achieved due to the fast interconversion between the monomeric and dimeric forms in solution. Other than Pc derivatives, few examples are known with supramolecular dimers bound by π−π interactions with high kinetic stability, such as the hexa-*peri*-hexabenzocoronenes (HBCs) with oligophenylene dendrons reported by Müllen *et al.*[35,36] or a tweezer-type perylene bisimide (PDI) reported by Würthner *et al.*[37] However, to the best of our knowledge, there are no examples of π-stacking molecules whose monomeric and dimeric forms are kinetically well-stabilized to be separated from each other. Hence, in this manuscript, we aimed to provide the first example of a Pc dimer bound by π−π interactions, which can be isolated from its monomer and handled as a single chemical entity. To obtain enough stabilization energy by π−π interactions, we conceived the idea to introduce wide π-systems perpendicularly arranged at the Pc periphery to use π−π interactions among the perpendicular π-systems in the dimer form (Fig. 1b). Recently, we have reported the synthesis of a phthalonitrile substituted with two 6,13-dihydro-6,13-diazapentacene (DHDAP) units (**2**), whose DHDAP moieties are fixed in a face-to-face manner and perpendicular to the benzene ring of phthalonitrile.[38] This molecule could be converted to Pcs with eight pillar-like DHDAP units (**1M**),

which can potentially form a tightly bound dimer (**1M2**) as shown in Fig. 1b. DFT calculations with the model compounds suggested that such dimers can be reasonably formed (see the ESI†). The stabilization energy for the dimerization was calculated to be −399.2 kJ mol^{-1}, and this value is much larger than that of **C** calculated at the same theoretical level (−321.5 kJ mol^{-1}).[34] In this work, we describe the synthesis and unique dimerization behavior of the zinc and copper Pcs, **1Zn** and **1Cu**.

Results and discussion

Synthesis

Two kinds of Pcs **1Zn** and **1Cu** were synthesized as examples of diamagnetic and paramagnetic ($S = 1/2$) Pcs according to Scheme 1. The precursor **2** was condensed in the presence of metal templates (Zn(OAc)$_2$ for **1Zn** and CuCl$_2$ for **1Cu**) and 1,8-diazabicyclo[5,4,0]undec-7-ene (DBU) by refluxing in 1-pentanol for 24 h. The reaction mixture was cooled down to room temperature and precipitated by adding methanol. The crude products were monitored by matrix-assisted laser desorption ionization time-of-flight mass spectrometry (MALDI-TOF-MS). Fig. 2a is the MALDI-TOF-MS spectrum of the crude product of the reaction with Zn(OAc)$_2$ as the metal template. The peaks derived from **1Zn2** were clearly observed along with the peaks of **1Zn**, and the peak intensity of **1Zn2** was much larger than that of **1Zn**. No peaks corresponding to the trimer or higher oligomers were found. The lack of the trimer and higher oligomers was understood from the structure of **1Zn2**, in which no spaces for the third monomer are left. The third monomer can have only minimal contact with **1Zn2** as understood from the molecular modeling of the trimer (Fig. S37†). We successfully isolated the dimers and monomers by recycling preparative gel permeation chromatography (GPC) (Fig. S1†). The MALDI-TOF-MS spectra of the first and the second eluting fractions unequivocally certified the isolation of **1Zn2** and **1Zn** (Fig. 2b and c). It is noteworthy to mention that no peaks derived from **1Zn** were observed from the measurements of isolated **1Zn2**, showing no dissociation of **1Zn2** during the ionization process of MALDI (Fig. 2b). The separation of **1Cu** and **1Cu2** was also accomplished in a similar way (Fig. S2†). We have done several trials and errors to obtain single crystals of these compounds, but unfortunately, only brittle crystals giving poor X-ray diffraction patterns were obtained in all cases. Therefore, the
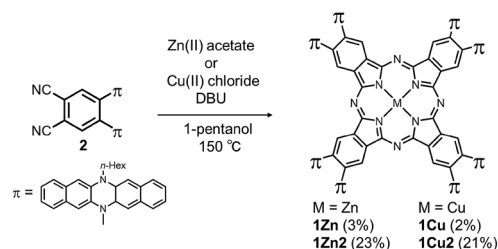
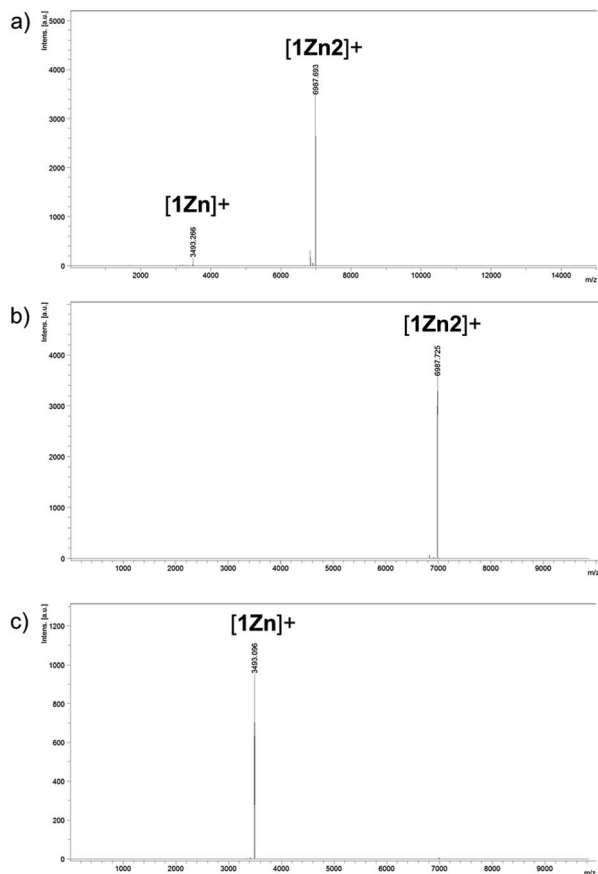

Scheme 1 Synthesis of target molecules.

Fig. 2 MALDI-TOF-MS spectra (positive) of (a) the reaction crude containing **1Zn** and **1Z2** and of (b) **1Zn2** and (c) **1Zn** isolated by HPLC.

structures of the dimers were investigated by combining various spectroscopic measurements as described below.

NMR spectroscopy

The structures of **1Zn** and **1Zn2** were thoroughly investigated using various 1D and 2D NMR techniques. The ^{1}H NMR spectrum of **1Zn** in tetrahydrofuran-d_8 shows seven peaks in the aromatic region (Fig. S4†). The protons of the benzo moieties of phthalocyanine were observed as a single peak at 10.27 ppm, and the other six peaks in the range of 6.3–7.1 ppm were attributed to the protons of the DHDAP units. The ^{13}C NMR spectrum of **1Zn** showed six aliphatic peaks and fourteen aromatic peaks (Fig. S5†). The results of ^{1}H and ^{13}C NMR spectra were fully consistent with the D_4 symmetric structure of **1Zn**. By combining the results of 1D and 2D NMR measurements, the peaks of DHDAP moieties of **1Zn** were successfully assigned as shown in Fig. 4a (details are shown in Fig. S6–S10†). The ^{1}H NMR spectrum of **1Zn2** in tetrahydrofuran-d_8 showed a greater number of peaks in the aromatic region than that observed in **1Zn** (Fig. S11†). The protons of the benzo moieties of **1Zn2** were also observed as a single peak at 10.27 ppm as in the case of **1Zn**, indicating the existence of a four-fold axis in **1Zn2**. The ^{13}C NMR spectrum of **1Zn2** showed six peaks of aliphatic carbons and twenty four peaks of aromatic carbons

(Fig. S12†). The HMQC measurements based on the result of the 1D ^{13}C NMR measurement clearly showed the existence of six different aliphatic protons and thirteen different aromatic protons in **1Zn2**, also being consistent with the interdigitated dimeric structure (Fig. S14†). Assuming the dimer structure shown in Fig. 1b, the outer (opposite side to the Pc of the complementary monomer) and inner (same side as the Pc of the complementary monomer) half of each DHDAP unit should be non-equivalent. Herein the protons of the inner naphthalene moiety of each DHDAP unit are labeled with apostrophes (a′ to f′), and all the protons of the DHDAP moieties were consistently assigned by combining the results of 1D and 2D NMR measurements as shown in Fig. 3b (details are shown in Fig. S13–S17†). The protons existing in the outermost part of the DHDAP units (b, c, and d) did not shift compared with those of **1Zn**, suggesting the negligible interaction from the other **1Zn** in the dimer. On the other hand, the protons of the inner half parts of DHDAP units (a′ to f′), which penetrate the pockets of the other monomer, showed significant shifts from those of **1Zn**. In particular, the protons c′ and d′ showed significant high-field shifts of 0.80 and 0.79 ppm respectively compared with those of **1Zn**. Judging from the optimized structure of the dimer, these protons exist above the π-plane of DHDAP of the other monomer, and the high-field shifts could be ascribed to the shielding effect from the DHDAP moiety. The protons f′ showed the largest down-field shift of 1.03 ppm compared with **1Zn** due to the strong deshielding effect from nearby Pc ring of the other monomer. The [1]H-DPFGSE-NOE spectra,[39] which
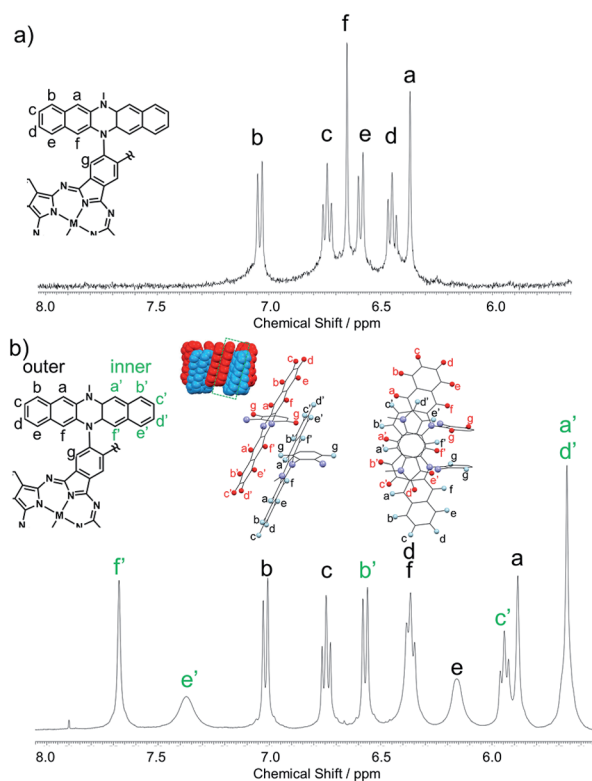

Fig. 3 Aromatic regions of ^{1}H NMR spectra for (a) **1Zn** and (b) **1Zn2** in tetrahydrofuran-d_8.

show weak NOE signals, also indicated the proposed dimer structure (Fig. S18†). We carried out DOSY measurements for a mixed solution of **1Zn** and **1Zn2** in tetrahydrofuran-d_8, and the diffusion constants of **1Zn** and **1Zn2** were evaluated to be 3.0×10^{-10} m^2 s^{-1} and 2.7×10^{-10} m^2 s^{-1}, respectively. The value for **1Zn2** was smaller than that for **1Zn**, but the difference was not so large. This result implies the compactly interdigitated structure of **1Zn2**.

ESR spectroscopy

Electron spin resonance (ESR) is a powerful tool to investigate the way of association of Pcs with a paramagnetic central metal such as Cu(II). To obtain further information about the dimer structure, we measured ESR spectra of the frozen solutions of **1Cu** and **1Cu2** in CH$_2$Cl$_2$. Fig. 4a shows the ESR spectrum of the frozen solution of **1Cu** in CH$_2$Cl$_2$ at 123 K. The spectral shape was a typical pattern of monomeric CuPcs[23,40] and well reproduced by spectral simulation using the axial g-value ($g_\parallel = 2.044$, $g_\perp = 2.164$), the hyperfine interaction from four equivalent nitrogen nuclei ($A_{iso}^N = 1.85$ mT) and one Cu nucleus ($A_\parallel^{Cu} = 3.06$ mT, $A_\perp^{Cu} = 21.6$ mT). On the other hand, a frozen solution of **1Cu2** showed a completely different spectral pattern (Fig. 4b). The transition for $\Delta M_s = \pm 1$ showed a characteristic fine structure of a triplet species with axial symmetry ($g_\parallel = 2.045$, $g_\perp = 2.081$, $D = 48.9$ mT, $E \simeq 0$ mT) in addition to the hyperfine splitting from two equivalent Cu nuclei ($A_\parallel^{Cu} = 1.40$ mT, $A_\perp^{Cu} =$

10.1 mT). Furthermore, the forbidden transition signal ($\Delta M_s = \pm 2$) with a seven-line splitting arises due to the two equivalent Cu nuclei ($I = 3/2$) in the half-field region, clearly indicating the spin–spin interaction between two CuPc moieties. The ESR spectral features of **1Cu** and **1Cu2** were completely in accordance with those of the monomers and H-type dimers of the crown ether substituted CuPcs,[23] definitely verifying the proposed dimer structure of **1Cu2**.

Electronic absorption spectra

Electronic absorption measurement is one of the important methods to obtain information about the mode of aggregation of dye molecules in solution. We measured the UV-vis-NIR absorption spectra of the monomeric and the dimeric Pcs in various solvents, and they showed different time evolutions of the absorption spectra depending on solvents. The solution of **1Zn** in tetrahydrofuran showed absorption bands corresponding to the Q-band of the Pc with a peak maximum at 675 nm and the bands ranging from 300 to 450 nm corresponding to the superposition of the absorption of DHDAP moieties and the Soret band of the Pc (Fig. 5). The solution of **1Zn2** in tetrahydrofuran also showed absorption bands ranging from 300 to 450 nm, similar to those of **1Zn** but the Q-band of **1Zn2** showed a hypsochromic shift to 652 nm, suggesting an H-type association of two Pc moieties (Fig. 5). Furthermore, the Q-band of **1Zn2** had a broad low-energy tail up to 1200 nm. It is important to note that the spectral shapes of both **1Zn** and **1Zn2** in tetrahydrofuran showed no temporal change over 72 h at room temperature, suggesting that both the dimerization of **1Zn** and the dissociation of **1Zn2** were negligible in tetrahydrofuran (Fig. S20†). The hypsochromic shift of the Q-band and the broad low-energy tail of **1Zn2** were observed in all the solvents tested, but the temporal changes of the absorption spectra depended on the solvents. In CH$_2$Cl$_2$, the absorption spectra of **1Zn** did not show any temporal change over 72 h at room temperature (Fig. 6a), whereas the absorption spectra of **1Zn2** slowly changed under the same conditions in the order of hours to days with isosbestic points at 659 nm and 890 nm (Fig. 6b). The original Q-band of **1Zn2** at 649 nm gradually decreased and a new peak at 677 nm emerged corresponding to the Q-band of
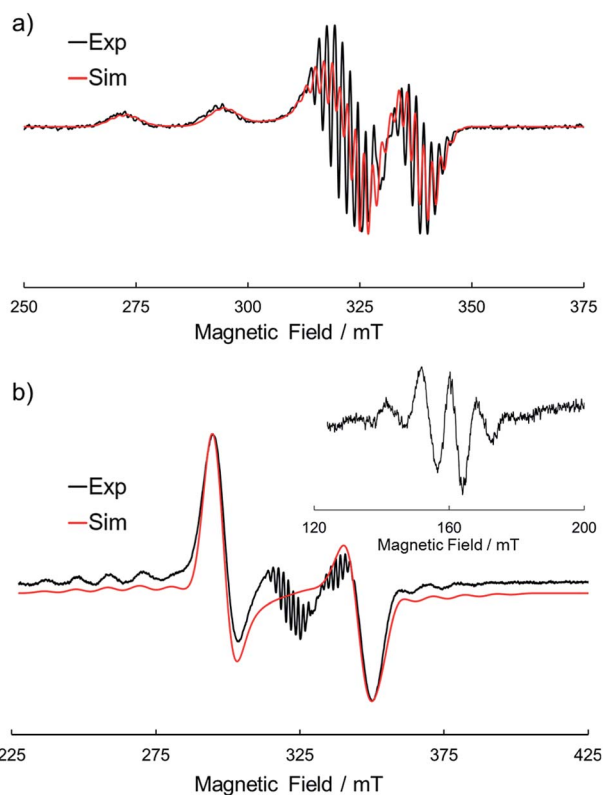

Fig. 4 ESR spectra of (a) **1Cu** and (b) **1Cu2** in CH$_2$Cl$_2$ at 123 K. The black and red lines represent the experimental and simulated spectra, respectively.
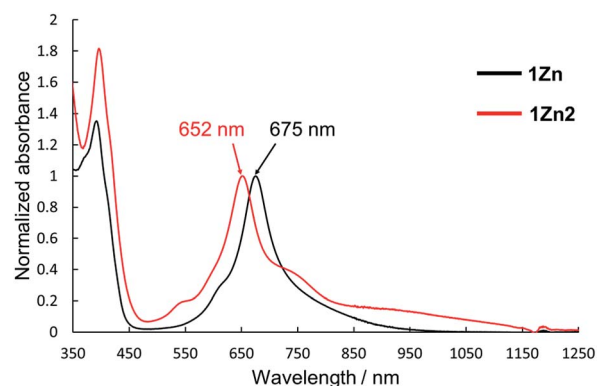

Fig. 5 UV-Vis-NIR absorption spectra of **1Zn** (1×10^{-5} M, black) and **1Zn2** (5×10^{-6} M, red) in tetrahydrofuran.
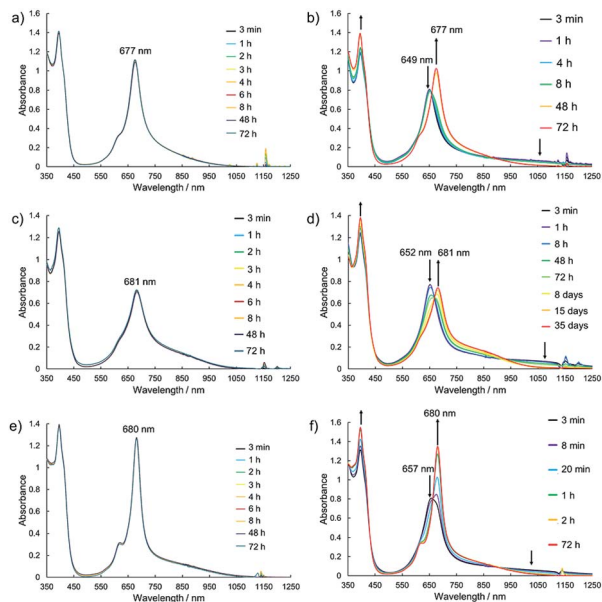
Fig. 6 Temporal changes of the UV-vis-NIR absorption spectra of **1Zn** (1 × 10^{-5} M) in (a) CH$_2$Cl$_2$, (c) toluene, and (e) o-dichlorobenzene and of **1Zn2** (5 × 10^{-6} M) in (b) CH$_2$Cl$_2$, (d) toluene, and (f) o-dichlorobenzene at room temperature.

Fig. 7 Temporal changes of the UV-vis-NIR absorption spectra of (a) **1Zn** (1 × 10^{-5} M) at 333 K and of (b) **1Zn2** (5 × 10^{-6} M) at room temperature in ethyl acetate.

1Zn, indicating the dissociation of **1Zn2** to **1Zn**. The spectral change of **1Zn2** in CH$_2$Cl$_2$ almost reached a steady state after 72 hours, and the spectral shape at this stage was completely in accordance with that of **1Zn** in CH$_2$Cl$_2$. In toluene, the solution of **1Zn** showed no temporal change (Fig. 6c) and **1Zn2** exhibited a similar dissociation behavior as in CH$_2$Cl$_2$, although the rate of dissociation was much slower (Fig. 6d). We found that the dissociation of **1Zn2** was remarkably accelerated in o-dichlorobenzene. The spectral shape of **1Zn2** in o-dichlorobenzene was almost completely changed to that of **1Zn** within 2 h (Fig. 6f), whereas the spectral shape of **1Zn** remains unchanged (Fig. 6e). The activation energy of the dissociation of **1Zn2** in o-dichlorobenzene was estimated to be about 72 kJ mol^{-1} from the Arrhenius plot by assuming a first-order reaction (Fig. S21 and S22†). The results in CH$_2$Cl$_2$, toluene, and o-dichlorobenzene indicate that the dimeric form is a metastable species and the monomeric state is thermodynamically favored, probably due to the strong solvation of the monomeric species. In particular, the faster dissociation in o-dichlorobenzene could be ascribed to the high affinity of o-dichlorobenzene for π-conjugated molecules, which can penetrate into the spaces between the interdigitated DHDAP moieties and break up the dimer bound by π–π interactions. On the other hand, different behaviors were observed in ethyl acetate. Interestingly, the solutions of both **1Zn** and **1Zn2** in ethyl acetate showed almost no changes at room temperature over 72 h (Fig. S23†). However, when the solution of **1Zn** in ethyl acetate was kept at 333 K, **1Zn** gradually dimerized and the spectral shape became similar to that of **1Zn2** after 15 h (Fig. 7). This result indicates that **1Zn** is metastable and **1Zn2** is thermodynamically favored in ethyl acetate. The activation energy of the dimerization of **1Zn** in ethyl acetate
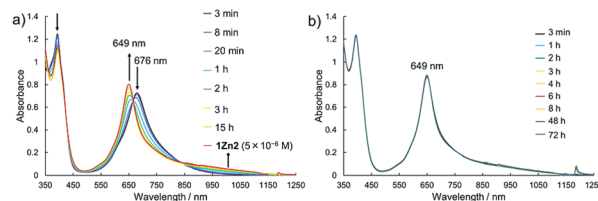
was estimated to be about 134 kJ mol^{-1} from the Arrhenius plot by assuming that the dimerization obeys a second-order reaction (Fig. S24 and S25†). Furthermore, **1Zn** also gradually dimerized in 1-pentanol, which was used as the reaction solvent in the final step of the synthesis, upon heating at 373 K (Fig. S26†). The fact that the yield of **1Zn2** was much higher than that of **1Zn** could be understood by this dimerization of **1Zn** during the reaction in the refluxing 1-pentanol. In tetrahydrofuran, the dimerization of **1Zn** was not observed even at 333 K (Fig. S27†), suggesting that both **1Zn** and **1Zn2** were kinetically well stabilized. The results of electronic absorption measurements of **1Cu** and **1Cu2** were similar to those of **1Zn** and **1Zn2** (Fig. S30–S35†).

Electrochemistry

To investigate the effect of the dimerization on the redox properties, electrochemical measurements were performed for **1Zn** and **1Zn2**. Fig. 8a shows the cyclic voltammogram (CV) and the differential pulse voltammogram (DPV) of **1Zn** in CH$_2$Cl$_2$ using [nBu$_4$N][BF$_4$] as the electrolyte. The oxidation processes were roughly grouped into three parts: ∼0 V, ∼0.25 V, and ∼0.9 V ($vs.$ ferrocene/ferrocenium), and the shapes of the voltammograms are basically similar to those of **2**.[38] In the CV measurement, **2** shows three reversible oxidation waves. The first and the second oxidation waves of **2** were assigned to the consecutive one-electron oxidation from each DHDAP unit at 0.10 and 0.28 V, and the third was assigned to the quasi two-electron oxidation from each DHDAP (0.82 and
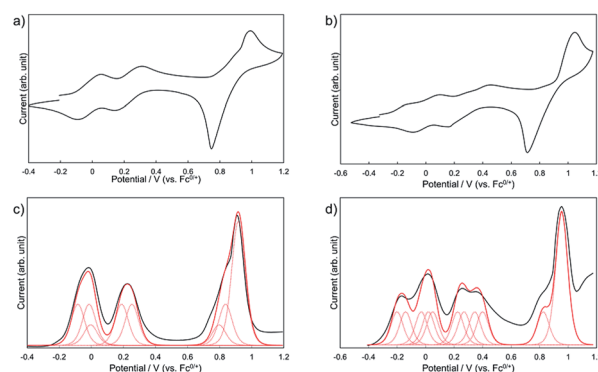

Fig. 8 Cyclic voltammograms of (a) **1Zn** and (b) **1Zn2** and differential pulse voltammograms of (c) **1Zn** and (d) **1Zn2** measured in CH$_2$Cl$_2$ containing 0.1 M [nBu$_4$N][BF$_4$] at 298 K (scan rate 100 m V s^{-1}).

Table 1 Oxidation potentials (V *vs.* ferrocene/ferrocenium) of **1Zn**, **1Zn2**, and **2** determined by the digital simulations of DPV in CH_2Cl_2 (0.1 M [nBu$_4$N][BF$_4$])

	E_1	E_2	E_3	E_4	E_5	E_6	E_7	E_8	E_9	E_{10}	E_{11}
1Zn	−0.08 (2e)	−0.01 (2e)	0.00 (1e)	0.19 (2e)	0.26 (2e)	0.80 (1e)	0.84 (2e)	0.92 (6e)			
1Zn2	−0.20 (2e)	−0.14 (2e)	−0.03 (2e)	0.02 (2e)	0.05 (2e)	0.23 (2e)	0.27 (2e)	0.35 (2e)	0.40 (2e)	0.83 (2e)	0.96 (8e)
2	0.10 (1e)	0.28 (1e)	0.82 (1e)	0.84 (1e)							

0.84 V), reflecting its twin donor structure. The similarity between the voltammograms of **1Zn** and **2** strongly indicates that the redox properties of **1Zn** could be attributed to the four independent co-facially stacked DHDAP pairs and one ZnPc, and actually the observed DPV of **1Zn** was well simulated by overlapping the oxidation waves of the four co-facially stacked DHDAP pairs like in **2** and the two one-electron oxidations of ZnPc at ~0 V and ~0.8 V (Fig. 8c). This result indicates that the electronic interaction among each co-facially stacked DHDAP pair in **1Zn** is small. The voltammograms of **1Zn2** in CH_2Cl_2, on the other hand, show more redox couples than **1Zn** (Fig. 8b). The DPV of **1Zn2** clearly showed the splitting of the first and second groups of the redox couples (Fig. 8d), suggesting the existence of through-space electronic communication among DHDAP pairs belonging to different monomers. Furthermore, the first oxidation potential showed a cathodic shift of 0.12 V, indicating the increased electron donating ability of **1Zn2** by forming the interdigitated dimer (Table 1).

Conclusions

We have prepared novel phthalocyanine (Pc) derivatives substituted with eight pillar-like DHDAP units on the periphery to maximize van der Waals interaction points and form selectively the H-type dimers of co-facial Pc rings. The dimers exhibited exceptional stability to be isolated from their monomeric forms in gel permeation chromatography protocols; even no dissociation was observed during the ionization process of MALDI-TOF-MS measurements. Both the monomers and dimers were well kinetically stabilized in solvents such as THF and ethyl acetate at room temperature and showed no temporal change over several days. In contrast, the dissociation of the dimers was observed in solvents with a high affinity for larger π-conjugated molecules such as *o*-dichlorobenzene. The meta-stable monomers were converted to the dimers by heating in solvents with less affinity for larger π-conjugated molecules such as ethyl acetate or 1-pentanol with a high activation energy of 134 kJ mol^{-1} in the former. The findings of this work will provide new molecular designs of supramolecular complexes and aggregates of π-conjugated molecules with an extremely strong bimolecular binding energy competitive to the chemical bonds by multi-point van der Waals interactions.

Conflicts of interest

There are no conflicts to declare.

Acknowledgements

Notes and references

1 *Phthalocyanines: Properties and Applications*, ed. C. C. Leznoff, and A. B. P. Lever, VCH, Weinheim, Germany, 1989, vol. 1–4.

2 C. G. Claessens, U. Hahn and T. Torres, *Chem. Rec.*, 2008, **8**, 75–97.

3 Z. Chen, A. Lohr, C. R. Saha-Möller and F. Würthner, *Chem. Soc. Rev.*, 2009, **38**, 564–584.

4 M. Kasha, H. R. Rawls and M. Ashraf El-Bayoumi, *Pure Appl. Chem.*, 1965, **11**, 371–392.

5 A. R. Monahan, J. A. Brado and A. F. DeLuca, *J. Phys. Chem.*, 1972, **76**, 446–449.

6 A. W. Snow and N. L. Jarvis, *J. Am. Chem. Soc.*, 1984, **106**, 4706–4711.

7 W. J. Schutte, M. Sluyters-Rehbach and J. H. Sluyters, *J. Phys. Chem.*, 1993, **97**, 6069–6073.

8 X.-F. Zhang, Q. Xi and J. Zhao, *J. Mater. Chem.*, 2010, **20**, 6726–6733.

9 N. Kobayashi, *Coord. Chem. Rev.*, 2002, **227**, 129–152.

10 C. C. Leznoff, S. Greenberg, S. M. Marcuccio, P. C. Minor, P. Seymour, A. B. P. Lever and K. B. Tomer, *Inorg. Chim. Acta*, 1984, **89**, L35–L38.

11 C. C. Leznoff, S. M. Marcuccio, S. Greenberg, A. B. P. Lever and K. B. Tomer, *Can. J. Chem.*, 1985, **63**, 623–631.

12 S. M. Marcuccio, P. I. Svirskaya, S. Greenberg, A. B. P. Lever, C. C. Leznoff and K. B. Tomer, *Can. J. Chem.*, 1985, **63**, 3057–3069.

13 E. S. Dodsworth, A. B. P. Lever, P. Seymour and C. C. Leznoff, *J. Phys. Chem.*, 1985, **89**, 5698–5705.

14 C. C. Leznoff, H. Lam, S. M. Marcuccio, W. A. Nevin, P. Janda, N. Kobayashi and A. B. P. Lever, *J. Chem. Soc., Chem. Commun.*, 1987, 699–701.

15 N. Kobayashi, H. Lam, W. A. Nevin, P. Janda, C. C. Leznoff, T. Koyama, A. Monden and H. Shirai, *J. Am. Chem. Soc.*, 1994, **116**, 879–890.

16 N. Kobayashi, T. Fukuda and D. Leliévre, *Inorg. Chem.*, 2000, **39**, 3632–3637.

17 C. C. Leznoff, H. Lam, W. A. Nevin, N. Kobayashi, P. Janda and A. B. P. Lever, *Angew. Chem., Int. Ed.*, 1987, **26**, 1021–1023.

18 Z. Odabaș, A. Altındal, A. R. Özkaya, M. Bulut, B. Salih and Ö. Bekaroğlu, *Polyhedron*, 2007, **26**, 695–707.

19 Y. Asano, A. Muranaka, A. Fukusawa, T. Hatano, M. Uchiyama and N. Kobayashi, *J. Am. Chem. Soc.*, 2007, **129**, 4516–4517.

20 A. R. Koray, V. Ahsen and Ö. Bekaroğlu, *J. Chem. Soc., Chem. Commun.*, 1986, 932–933.

21 N. Kobayashi and Y. Nishiyama, *J. Chem. Soc., Chem. Commun.*, 1986, 1462–1463.

22 R. Hendriks, O. E. Sielcken, L. A. Van de Kuil, W. Drenth and R. J. M. Nolte, *J. Chem. Soc., Chem. Commun.*, 1986, 1464–1465.

23 N. Kobayashi and A. B. P. Lever, *J. Am. Chem. Soc.*, 1987, **109**, 7433–7441.

24 T. F. Baumann, A. G. M. Barrett and B. M. Hoffman, *Inorg. Chem.*, 1997, **36**, 5661–5665.

25 S. J. Lange, H. Nie, C. L. Stern, A. G. M. Barrett and B. M. Hoffman, *Inorg. Chem.*, 1998, **37**, 6435–6443.

26 N. Kobayashi, A. Muranaka and V. N. Nemykin, *Tetrahedron Lett.*, 2001, **42**, 913–915.

27 K. Kameyama, M. Morisue, A. Satake and Y. Kobuke, *Angew. Chem., Int. Ed.*, 2005, **44**, 4763–4766.

28 M. V. Martínez-Díaz, M. S. Rodrígues-Morga, M. C. Feiters, P. J. van Kan, R. J. M. Nolte, J. F. Stoddart and T. Torres, *Org. Lett.*, 2000, **2**, 1057–1060.

29 Y. Yamada, M. Okamoto, K. Furukawa, T. Kato and K. Tanaka, *Angew. Chem., Int. Ed.*, 2012, **51**, 709–713.

30 M. Morisue, S. Ueda, M. Kurasawa, M. Naito and Y. Kurida, *J. Phys. Chem. A*, 2012, **116**, 5139–5144.

31 C. A. Hunter and J. K. Sanders, *J. Am. Chem. Soc.*, 1990, **112**, 5525–5534.

32 G. Bottari, O. Trukhina, A. Kahnt, M. Frunzi, Y. Murata, A. Rodríguez-Fortea, J. M. Poblet, D. M. Guldi and T. Torres, *Angew. Chem., Int. Ed.*, 2016, **55**, 11020–11025.

33 N. Kobayashi, Y. Kobayashi and T. Osa, *J. Am. Chem. Soc.*, 1993, **115**, 10994–10995.

34 K. Wang, D. Qi, H. Wang, W. Cao, W. Li and J. Jiang, *Chem.–Eur. J.*, 2012, **18**, 15948–15952.

35 J. Wu, M. D. Watson and K. Müllen, *Angew. Chem., Int. Ed.*, 2003, **42**, 5329–5333.

36 J. Wu, A. Fechtenkötter, J. Gauss, M. D. Watson, M. Kastler, C. Fechtenkötter, M. Wagner and K. Müllen, *J. Am. Chem. Soc.*, 2004, **126**, 11311–11321.

37 C. Shao, M. Stolte and F. Würthner, *Angew. Chem., Int. Ed.*, 2013, **52**, 7482–7486.

38 D. Sakamaki, H. Saeki and S. Seki, *Mater. Chem. Front.*, 2018, **2**, 530–536.

39 K. Stott, J. Stonehouse, J. Keeler, T.-L. Hwang and A. J. Shaka, *J. Am. Chem. Soc.*, 1995, **117**, 4199–4200.

40 C. M. Guzy, J. B. Raynor and M. C. R. Symons, *J. Chem. Soc. A*, 1969, 2299–2303.